

## Step-bunched Bi-terminated Si(111) surfaces as a nanoscale orientation template for quasisingle crystalline epitaxial growth of thin film phase pentacene

Toshihiro Shimada,<sup>1,a)</sup> Manabu Ohtomo,<sup>1</sup> Tadamasu Suzuki,<sup>1</sup> Tetsuya Hasegawa,<sup>1</sup> Keiji Ueno,<sup>2</sup> Susumu Ikeda,<sup>3</sup> Koichiro Saiki,<sup>3</sup> Miho Sasaki,<sup>4</sup> and Katsuhiko Inaba<sup>4</sup>

<sup>1</sup>Department of Chemistry, The University of Tokyo, Bunkyo-ku, Tokyo 113-0033, Japan

<sup>2</sup>Department of Chemistry, Saitama University, Saitama 338-8570, Japan

<sup>3</sup>Department of Complexity Sciences and Engineering, The University of Tokyo, Kashiwa 277-8561, Japan

<sup>4</sup>Rigaku Corporation, 3-9-12 Matsubara-cho, Akishima, Tokyo 196-8666, Japan

(Received 23 September 2008; accepted 11 November 2008; published online 2 December 2008)

We developed a nanoscale orientation template for quasisingle crystalline epitaxial growth of thin film phase pentacene. By using  $\alpha\text{-}\sqrt{3}\times\sqrt{3}$  Bi termination of surface dangling bonds on step-bunched vicinal surface of Si(111), thin film phase epitaxial pentacene was grown with the crystal axes aligned to the surface steps. Alignment occurred when the step height was higher than the molecular height. The mechanism of the alignment was examined by calculating the energy of the crystal edge. © 2008 American Institute of Physics. [DOI: 10.1063/1.3040309]

Controlling the molecular orientation in organic thin films is quite useful for various purposes such as polarized electroluminescence,<sup>1</sup> high mobility transistors,<sup>2</sup> and the band structure determination by angle resolved photoemission.<sup>3</sup> However, epitaxial growth of organic molecules on a single crystalline inorganic substrate is not sufficient in most cases. Since the crystal lattice of organic molecules usually has a symmetry lower than the substrate surface, there are several equivalent orientations of the organic lattices placed on the surface. This symmetry mismatch produces multiple-oriented domain structures, and the resulting film becomes useless in terms of the orientation-dependent applications or measurements. Applicability of organic epitaxial growth is currently rather limited because of this difficulty. In the present study, we report the preparation of surfaces with a lower symmetry using the step bunching of Si(111) and dangling-bond termination<sup>4</sup> and demonstrate the quasisingle crystalline growth of a monolayer (ML) pentacene with a *thin film phase*, which is widely used in thin film transistors (TFTs).

Pentacene is one of the most important organic semiconductors for TFT applications due to its high carrier mobility in thin films. Since the electronic conduction occurs through the interaction of  $\pi$ -electrons, which extends perpendicular to the long axis, it is essential to grow a film with the molecular long axis perpendicular to the surface (standing orientation) for its successful application. The orientation of the molecules is strongly dependent on the electronic structure of the substrate surface.<sup>5</sup>

Several groups, including us, found that the epitaxial growth of pentacene in the standing orientation occurs on hydrogen-terminated Si(111) (Ref. 6) and Bi(001) films formed on Si(111),<sup>7</sup>  $\sqrt{3}\times\sqrt{3}$  Bi-terminated Si(111),<sup>8,9</sup> but the epitaxial film is composed of domains with six equivalent in-plane crystal orientations, which are a major obstacle in the fundamental studies, such as the precise analysis of the orientation-dependent measurements.<sup>10</sup> Since vicinal surfaces of single crystals, such as Si(111), have regularly

spaced steps with an atomic order height, they are sometimes used as a template<sup>11-14</sup> for controlling the growth of organic thin films in a manner similar to graphoepitaxy of organic molecules.<sup>15,16</sup> A larger periodic structure formed by step bunching can also be used for orientation of the polymer chains.<sup>17</sup>

We tried to find a surface satisfying the following conditions: (1) suitable for the epitaxial growth of pentacene with a “standing orientation” and (2) with surface steps whose spacing and height are tunable by the preparation conditions. We focused on the step bunching of vicinally cut Si(111) surfaces because the height and the spacing of the periodic structure can be controlled by carefully tuning the annealing and cooling conditions.<sup>18</sup> Since clean surfaces of Si(111) are not suitable for the epitaxial growth of pentacene due to dangling bonds on the surfaces, we examined the possibility of using the Bi-terminated Si(111) while maintaining the surface morphologies of bunched steps.

Si(111) miscut nominally by  $2^\circ$  in the  $\langle\bar{1}\bar{1}2\rangle$  direction was used to prepare the regularly spaced steps on the surface. A flat surface with a miscut angle less than  $\pm 0.2^\circ$  was also used for comparison. A clean surface of Si(111) was obtained by flash heating the substrate up to  $1250^\circ\text{C}$ , followed by cooling to room temperature using a variable cooling rate in an ultrahigh vacuum. Bi thin films were deposited on the surface with several ML coverage. The coverage of the Bi films was monitored by reflection high-energy electron diffraction (RHEED) images and a quartz crystal microbalance. The Bi-covered Si(111) surface with steps was annealed to make various superstructures induced by Bi. The results using the substrate with a brief annealing to  $450^\circ\text{C}$  are now presented. The intensity versus incident electron energy ( $I$ - $V$ ) characteristics of low-energy electron diffraction (LEED) from this substrate agree with the  $\alpha$ -phase of  $\sqrt{3}\times\sqrt{3}$  Bi-Si(111),<sup>19</sup> which has a  $1/3$  ML coverage of Bi atoms. Epitaxial growth of the pentacene did not occur on the  $\beta$ -phase  $\sqrt{3}\times\sqrt{3}$  Bi-Si(111), which has full ML coverage of Bi atoms on the surface Si and is formed at a lower annealing temperature. The sample surface was *in situ* examined by

<sup>a)</sup>Electronic mail: shimada@chem.s.u-tokyo.ac.jp.

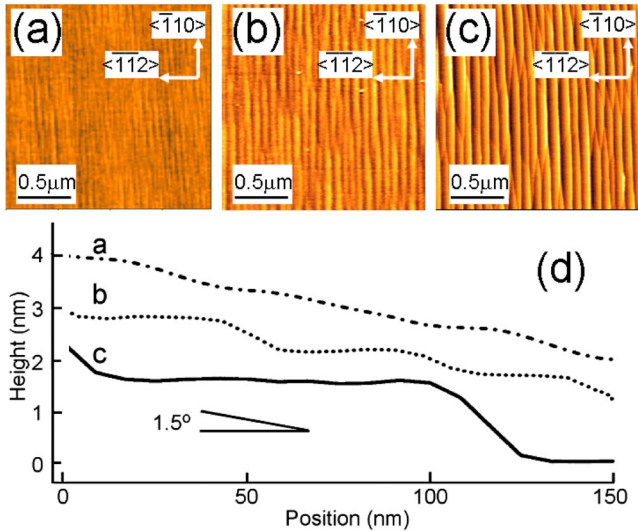


FIG. 1. (Color online) AFM images of Bi-terminated Si(111)  $2^\circ$ -off substrates with step bunching prepared at various cooling rates: (a) quench ( $>50^\circ\text{C}/\text{min}$ ), (b)  $20^\circ\text{C}/\text{min}$ , and (c)  $5^\circ\text{C}/\text{min}$ . (d) shows the cross sectional plots for (a)–(c).

RHEED and LEED, followed by *ex situ* atomic force microscopy (AFM) and surface x-ray diffraction (SXRD) observations.

Figure 1 shows the AFM image of the  $\alpha$ -phase  $\sqrt{3} \times \sqrt{3}$  Bi-Si(111) substrate prepared from the  $2^\circ$  miscut Si wafers. A different surface morphology was obtained depending on the cooling rate after flashing. The conditions of the cooling rate after flash heating included quenching  $>50^\circ\text{C}/\text{min}$  [Fig. 1(a)],  $20^\circ\text{C}/\text{min}$  [Fig. 1(b)], and  $5^\circ\text{C}/\text{min}$  [Fig. 1(c)], respectively. In Figs. 1(a)–1(c), the average step height of the sample was about 0.5, 1, and 3 nm, respectively. It should be noted that the surface periodic structure is controlled by step bunching and the surface step structure is maintained after termination by the Bi superstructure.

The sub-ML pentacene was deposited using these surface step structures as substrates. Temperature of the substrate was maintained at  $80^\circ\text{C}$  during the deposition. This was the optimum growth temperature. Lower temperature frequently yielded amorphous films and the sticking coefficient substantially decreased at higher temperature. Figure 2 shows the AFM images and RHEED patterns of the substrate after the pentacene deposition. Figure 2(a) shows the AFM image of the pentacene film grown on the surface with the average step height of less than 0.5 nm. It shows a corrugated profile with the third layer on top of the domains covering small areas. Based on this result, it is suggested that the wettability is controlled by the existence of the appropriately controlled steps.

The substrate used in Figs. 2(b) and 2(c) was made using the same conditions as in Figs. 1(b) and 1(c), respectively. The thickness of the sub-ML pentacene in these images is estimated to be about 1.5 nm, which is similar to the length of the long axis of the pentacene molecule. This indicates that the sub-ML pentacene has a “standing” orientation. In Fig. 2(c), it is clearly seen that the growth of the pentacene ML is affected by the periodic steps on the substrate. To examine the structures of the pentacene thin films, the RHEED image of the sub-ML pentacene was observed. Fig-

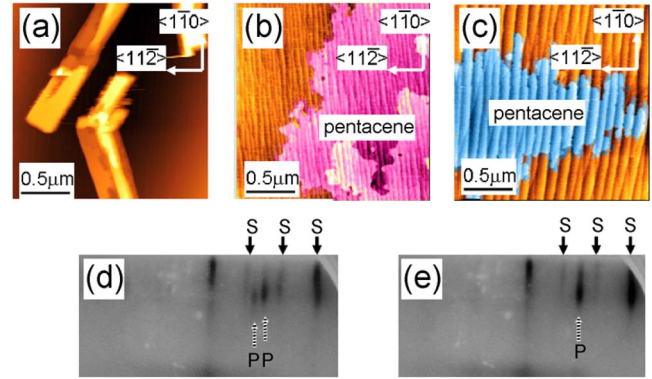


FIG. 2. (Color online) [(a)–(c)] AFM images of sub-ML pentacene grown on step-bunched substrates corresponding to Fig. 1. [(d) and (e)] RHEED images corresponding to (b) and (c), respectively. *S* and *P* denote the diffraction from the substrates and pentacene, respectively. The incident energy and the azimuth of the electron beam were 5 keV and along the  $\text{Si}\langle 1\bar{1}2 \rangle$ , respectively.

ures 2(d) and 2(e) are the RHEED images of the sub-ML pentacene shown in Figs. 2(b) and 2(c), respectively. The electron beam incident azimuth was along the  $\text{Si}\langle 11\bar{2} \rangle$ . The RHEED image corresponding to Fig. 2(a) was spotty but similar to Fig. 2(b). Two streaks of pentacene are observed between the streaks of substrate in Fig. 2(d), while only one streak of pentacene is observed between the streaks of the substrate in Fig. 2(e). These results indicate that the sub-ML pentacene in Fig. 2(c) has a single orientation in terms of the RHEED observation, whereas the sub-ML pentacene in Figs. 2(a) and 2(b) has multiple orientations.

To more precisely determine the lattice parameters of sub-ML pentacene in Fig. 2(c), LEED observations were carried out. For comparison, Fig. 3(a) shows the LEED image of pentacene grown on the atomically flat  $\alpha$ -phase  $\sqrt{3} \times \sqrt{3}$  Bi-Si(111) with a sub-ML coverage. As seen in the indices shown in Fig. 3(a), there are at least three equivalent orientations of the pentacene lattice due to the symmetry mismatch. Figure 3(b) shows the LEED image of the sub-ML pentacene shown in Fig. 2(c). The diffraction spots of pentacene form a singly oriented orthogonal shape. It can be seen that each diffraction spot splits into two. In order to improve the resolution, the diffraction pattern of the same sample was observed using SXRD by a RIGAKU ATX-G diffractometer under ambient conditions. The pentacene 11 diffraction peak was clearly observed and the split was  $3.5^\circ$  [Fig. 3(c)]. The lattice parameters determined from the LEED and SXRD were  $a=0.593$  nm,  $b=0.759$  nm, and  $\gamma=90^\circ$ , which coincide with the thin film phase rather than the other polymorphs of pentacene.<sup>20,21</sup>

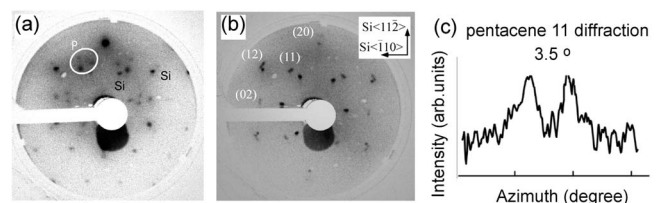


FIG. 3. (a) LEED patterns of sub-ML pentacene films on (a) flat and (b) step-bunched  $\sqrt{3} \times \sqrt{3}$  Bi-Si(111). (c) SXRD of pentacene 11 peak of pentacene grown on step-bunched Bi-Si(111). *P* in (a) denotes diffraction from pentacene.

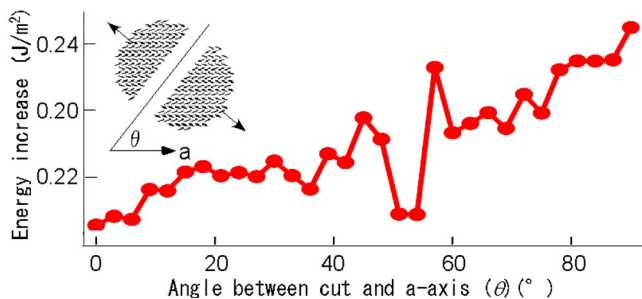


FIG. 4. (Color online) Energy increase when a cut is created in a pentacene ML disk shown in the inset plotted as a function of the angle.

As for the mechanism of the lattice alignment by the steps, we consider that there are three possibilities. The first one is the energy of truncation. The ML crystal of pentacene is truncated at the step edge of the substrate and this makes the total energy increase due to the “surface energy” at the edge. The second one is the interaction between the step wall and the molecular film. The third one is the kinetic effect, which affects the molecular motion<sup>22</sup> and controls the domain shape.<sup>13</sup> In order to examine these possibilities, we estimated the surface energy increase ( $\Delta E$ ) when the crystal is cut at various azimuths using a method similar to that in Ref. 23. Figure 4 shows  $\Delta E$  plotted versus the angle from the  $a$ -axis ( $\theta$ ). The energy was calculated using the force field MM3, which is frequently used for estimation of the van der Waals energy of the aromatic crystal. The interaction with the substrate was neglected. It was found that the minimum energy increase is observed when the truncation occurs parallel to the  $a$ -axis ( $\theta=0^\circ$ ) and a dip is observed at  $\theta=53^\circ$ , which corresponds to the truncation parallel to the (110) face of pentacene. In the experiment, the alignment occurred parallel to the  $b$ -axis, which was the most unfavorable in terms of the energy increase induced by the truncation. This result rules out the contribution of the truncation energy. Although the precise structure of the Bi-terminated step wall is not known at present, we noticed that the pentacene domain shown in Fig. 2(c) continues beyond the bunched steps. This was commonly observed, and we presume that the bunched step has a finite slope to make the orientation information continue. We consider that the interaction at this part is important and thermodynamically governs the orientation of the nuclei or kinetically controls the growth speed of the domains.

In conclusion, we developed a nanoscale template for the quasisingle crystalline orientation of the thin film phase pentacene. Our method is a combination of step bunching of the vicinally cut substrate and proper surface termination. The mechanism was examined by calculating the energy in-

crease by truncation at the edge and it is concluded that the interaction between the step wall and the molecules is important for the alignment.

The present work was partly supported by KAKENHI (17260008, 19651048) from MEXT and the JST “Seeds Innovation Program”.

- <sup>1</sup>M. Misaki, Y. Ueda, S. Nagamatsu, Y. Yoshida, N. Tanigaki, and K. Yase, *Appl. Phys. Lett.* **87**, 243503 (2005).
- <sup>2</sup>D. J. Gundlach, J. E. Royer, S. K. Park, S. Subramanian, O. D. Jurchescu, B. H. Hamadani, A. J. Moad, R. J. Klimm, L. C. Teague, O. Kirillov, C. A. Richter, J. G. Kushmerick, L. J. Richter, S. R. Parkin, T. N. Jackson, and J. E. Anthony, *Nature Mater.* **7**, 216 (2008).
- <sup>3</sup>G. Koller, S. Berkebile, M. Oehzelt, P. Puschniq, C. Ambrosch-Draxl, F. P. Netzer, and M. G. Ramsey, *Science* **317**, 351 (2007).
- <sup>4</sup>F. Meyer zu Heringdorf, M. C. Reuter, and R. M. Tromp, *Nature (London)* **412**, 517 (2001).
- <sup>5</sup>G. E. Thayer, J. T. Sadowski, F. Meyer zu Heringdorf, T. Sakurai, and R. M. Tromp, *Phys. Rev. Lett.* **95**, 256106 (2005).
- <sup>6</sup>T. Shimada, H. Nogawa, T. Hasegawa, K. Ueno, and K. Saiki, *Appl. Phys. Lett.* **87**, 061917 (2005).
- <sup>7</sup>J. T. Sadowski, T. Nagao, S. Yaginuma, Y. Fujikawa, A. Al-Manboob, K. Nakajima, T. Sakurai, G. E. Thayer, and R. M. Tromp, *Appl. Phys. Lett.* **86**, 073109 (2005).
- <sup>8</sup>T. Suzuki, T. Shimada, K. Ueno, S. Ikeda, K. Saiki, and T. Hasegawa, *Organic Electronics—Materials, Devices and Applications*, MRS Symposium Proceedings No. 965 (Materials Research Society, Pittsburg, 2007), pp. S06–19.
- <sup>9</sup>A. Al-Mahboob, J. T. Sadowski, Y. Fujikawa, K. Nakajima, and T. Sakurai, *Phys. Rev. B* **77**, 035426 (2008).
- <sup>10</sup>H. Kakuta, T. Hirahara, I. Matsuda, T. Nagao, S. Hasegawa, N. Ueno, and K. Sakamoto, *Phys. Rev. Lett.* **98**, 247601 (2007).
- <sup>11</sup>T. Shimada, A. Suzuki, T. Sakuada, and A. Koma, *Appl. Phys. Lett.* **68**, 2502 (1996).
- <sup>12</sup>M. Nakamura, T. Matsunobe, and H. Tokumoto, *J. Appl. Phys.* **89**, 7860 (2001).
- <sup>13</sup>S. Nishikata, G. Sazaki, T. Terauchi, N. Usami, S. Suto, and K. Nakajima, *Cryst. Growth Des.* **7**, 439 (2007).
- <sup>14</sup>V. Ignatescu, J. C. M. Hsu, A. C. Mayer, J. M. Blakely, and G. G. Malliaras, *Appl. Phys. Lett.* **89**, 253116 (2006).
- <sup>15</sup>S. Ikeda, K. Saiki, K. Tsutsui, T. Edura, Y. Wada, H. Miyazoe, K. Terashima, K. Inaba, T. Mitsunaga, and T. Shimada, *Appl. Phys. Lett.* **88**, 251905 (2006).
- <sup>16</sup>S. Ikeda, K. Saiki, Y. Wada, K. Inaba, Y. Ito, H. Kikuchi, K. Terashima, and T. Shimada, *J. Appl. Phys.* **103**, 084313 (2008).
- <sup>17</sup>R. Onoki, S. Abe, K. Ueno, H. Nakahara, and K. Saiki, *Chem. Lett.* **35**, 746 (2006).
- <sup>18</sup>F. K. Men, F. Liu, P. J. Wang, C. H. Chen, D. L. Cheng, J. L. Lin, and F. J. Himpsel, *Phys. Rev. Lett.* **88**, 096105 (2002).
- <sup>19</sup>K. J. Wan, T. Guo, W. K. Ford, and J. C. Hermanson, *Surf. Sci.* **261**, 69 (1992).
- <sup>20</sup>S. E. Fritz, S. M. Martin, C. D. Frisbie, M. D. Ward, and M. F. Toney, *J. Am. Chem. Soc.* **126**, 4084 (2004).
- <sup>21</sup>H. Yoshida, K. Inaba, and N. Sato, *Appl. Phys. Lett.* **90**, 181930 (2007).
- <sup>22</sup>T. Shimada, H. Ichikawa, and K. Saiki, *Appl. Phys. Lett.* **89**, 141912 (2006).
- <sup>23</sup>S. Verlaak, C. Rolin, and P. Heremans, *J. Phys. Chem. B* **111**, 139 (2007).